Testing the SOLPS-ITER drift model in Ohmic TCV discharges

C. Colandrea[1], H. Reimerdes[1], M. Wensing[1], H. De Oliveira[1], B. P. Duval[1], O. Février[1], S. Gorno[1], B. L. Linehan[2], L. Martinelli[1], A. Perek[3], C. K. Tsui[1], C. Theiler[1], M. Wischmeier[4], the EUROfusion MST1 team* and the TCV team †

[1] *École Politechnique Fédérale de Lausanne- Swiss Plasma Center, Lausanne, Switzerland*
[2] *Massachusetts Institute of Technology, Cambridge, MA, USA*
[3] *Dutch Institute for Fundamental Energy Research, Eindhoven, The Netherlands*
[4] *Max-Planck- Institut für Plasmaphysik, Garching, Germany*

This contribution investigates drift effects on the scrape-off-layer transport of particles and heat in the TCV tokamak using experiments with both toroidal magnetic field B_t directions and the SOLPS-ITER code [1]. The drift model in the code is tested through stringent comparison with TCV measurements, employing several edge diagnostics that include Bolometry (BOLO), Infrared Thermography (IR), Thomson scattering (TS), Divertor Spectroscopy System (DSS), Langmuir Probes (LP). Although a satisfactory qualitative agreement for multiple diagnostics is seen, several quantitative mismatches remain, whose explanation requires further investigation.

Simulation setup and comparison strategy

SOLPS-ITER drift simulations are performed for Ohmically heated, density ramp TCV discharges with divertor baffles and current $I_p = 190$ kA, which is the largest current that allows a comparison of both B_t directions in the L-mode regime (Fig.1). Spatially uniform particle and thermal diffusivities, $D_\perp^{AN} = 0.1 m^2/s$, $\chi_{i,\perp}^{AN} = 0.1 m^2/s$, $\chi_{e,\perp}^{AN} = 0.7 m^2/s$, are chosen to best fit the experimental radial density and temperature fall-off lengths at the outer midplane, obtained with the fast reciprocating probe (RCP), for a reference density case. The gas puff rate Γ_{puff} is varied from 5 to $15 \cdot 10^{20} D_2/s$ for a comparison with TCV data at multiple times during the density ramp. The power crossing the separatrix $P_{sep} \approx 200kW$ is kept constant, as an increase of the Ohmic power with density is compensated by higher core radiation.

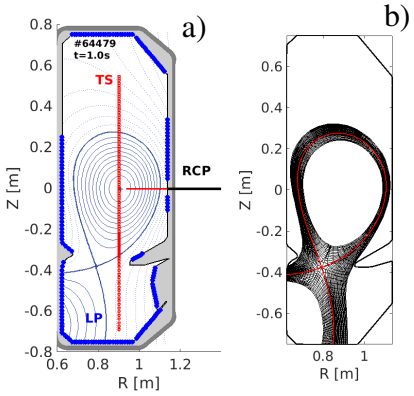

Figure 1: Reference discharge magnetic geometry and main diagnostics a), simulation grid b).

A comparison of simulation with experiment requires an ordering parameter to link simulation and experimental time intervals. The separatrix density at the outboard midplane is not suitable as the RCP measurements are too sparse in time. The separatrix density at the divertor entrance

*See author list of B. Labit et al 2019 Nucl. Fusion **59** 086020
†See author list of S. Coda et al 2019 Nucl. Fusion **59** 112023

$n_{e,sep}^{div\text{-}e}$, measured with Thomson scattering, is again not a suitable general ordering parameter since it exhibits a roll-over at high core density (Fig.2) and is, therefore, not unique. The simulated $n_{e,sep}^{div\text{-}e}$ does not exhibit a roll-over, where increased gas fuelling always increases $n_{e,sep}^{div\text{-}e}$. The line-average density $\langle n_e \rangle_l$, measured with the Far-infrared interferometer, is chosen as ordering parameter, following the approach in [2]. For each simulation, a value of $\langle n_e \rangle_l$ is assigned, based on the fitted relation $n_{e,sep}^{div\text{-}e} \approx 0.3 \langle n_e \rangle_l$ (Fig.2). The analysis is, therefore, restricted to time intervals where the linearity between $n_{e,sep}^{div\text{-}e}$ and $\langle n_e \rangle_l$ is obtained.

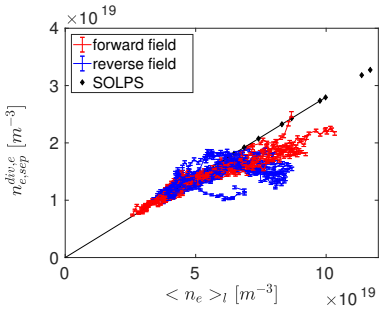

Figure 2: Separatrix density at lower TS-separatrix intersection $n_{e,sep}^{div\text{-}e}$ as a function of the line-averaged density $\langle n_e \rangle_l$.

Divertor entrance

The electron density n_e and temperature T_e profiles are measured byThomson scattering at the lower separatrix intersection, which corresponds to the divertor entrance (Fig.1a). While the simulations reproduce the measured fall-off length within the uncertainty of the measurement in forward field, they predict a non-monotonic n_e radial profile in reversed field, which is not observed experimentally (Fig.3c). In addition, simulations generally overestimate the separatrix temperature $T_{e,sep}$ (Fig.3b,d).

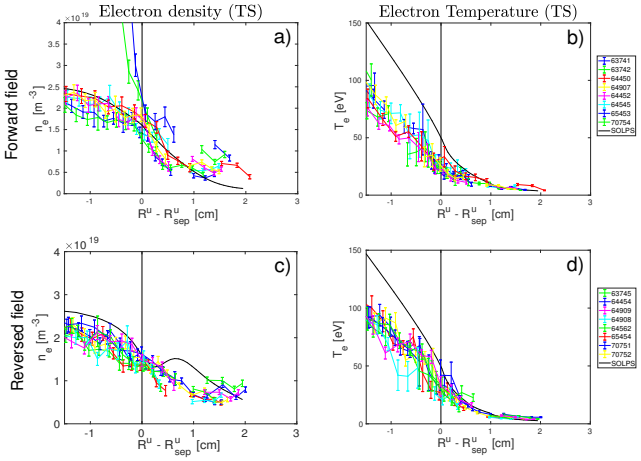

Figure 3: TS electron density n_e / temperature T_e in forward (a,b) and reversed (c,d) field. $\langle n_e \rangle_l = 5.1 \cdot 10^{19} m^{-3}$

SOL radiation and carbon emission

Bolometers are used to reconstruct the 2D spatial distribution of the radiation emissivity. The radiated power in the SOL P_{rad}^{SOL} is then estimated using the magnetic equilibrium reconstruction. In forward field, the experimental power radiated in the SOL increases with $\langle n_e \rangle_l$ and saturates (Fig.4a), albeit at different values of density. In reversed field, an indication of saturation is present at higher $\langle n_e \rangle_l$ than for forward field (Fig.4b). The simulated P_{rad}^{SOL} saturates around $\langle n_e \rangle_l \approx 7 \cdot 10^{19} m^{-3}$. A decrease in upstream and divertor temperatures with $\langle n_e \rangle_l$ is among the effects that may be responsible for this radiated power saturation (Fig.4).

The development of a synthetic DSS [2] allows for a direct comparison with DSS line-integrated

measurements. To examine the carbon content and test the simulated carbon source, the CII 426.8 nm and CIII 465.0 nm spectral lines are compared. In contrast with BOLO results, the carbon line emissions from the synthetic DSS exceed the measurements by a factor of 2-5, with the greater discrepancy between simulation and experiment in forward field, for both C lines (Fig.4b,c). The comparison with BOLO and DSS systems suggests that simulations overestimate the carbon content or that there are more favorable conditions for C radiation in the divertor, despite the good agreement in the total radiated power.

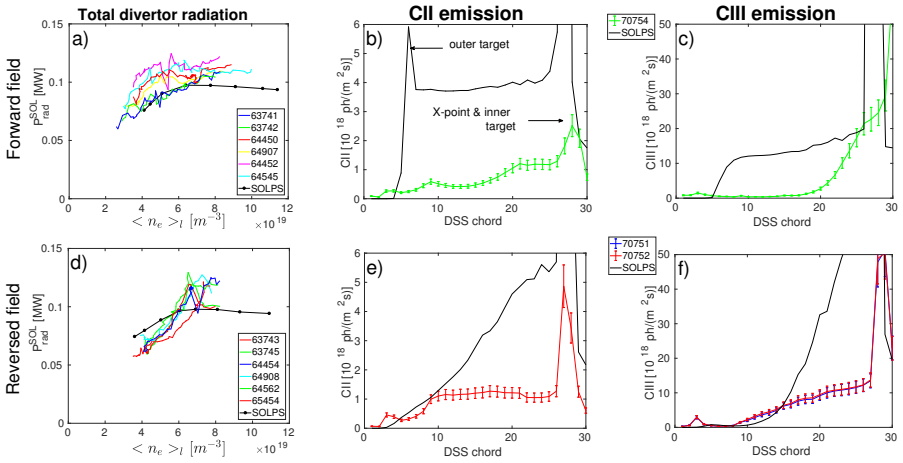

Figure 4: BOLO radiated power in the SOL P_{rad}^{SOL} in forward a) and reversed d) field. CII 426.8 nm /CIII 465.0 nm line brightness in forward (b,c) and reversed field (e,f) from DSS. Chord 1 intercepts the floor at R$\sim$ 1m; chord 30 intercepts the X-point and inner target. $\langle n_e \rangle_l = 5.1 \cdot 10^{19} m^{-3}$.

Target profiles

The target plasma parameters are inferred from Langmuir probes (target currents, electron density and temperature) and Infrared thermography (heat flux). Target current measurements with wall-mounted Langmuir probes biased to machine potential, show that the TCV divertor is dominated by Pfirsch-Schlüter flows [3]. Drift simulations reproduce the salient features of the observed profiles (Fig.5). The simulations overestimate the electron density at both targets and for both B_t directions by a factor 3-5. At the inner target, the simulated n_e radial profile exhibits a double peak (Fig.6a), which was found in previous drift simulations and experiments [4]. At the outer target, the simulated n_e profile is radially shifted towards the Private Flux Region in the forward field case and towards the Common Flux Region in the reversed field case (Fig.6b). While a double-peaked profile at the inner target is not seen

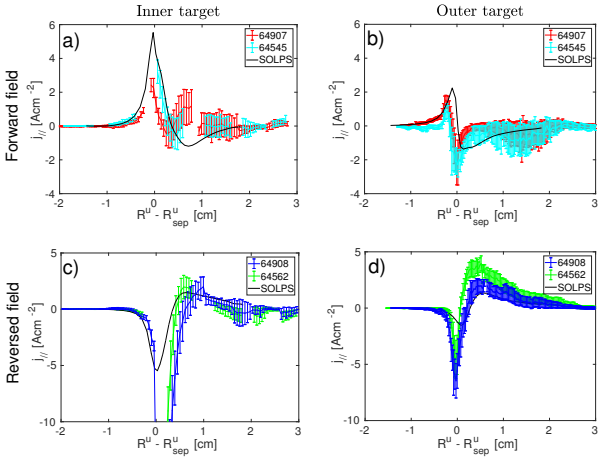

Figure 5: LP parallel target current in forward (a,b) and reversed (c,d) field. $\langle n_e \rangle_l = 6.2 \cdot 10^{19} m^{-3}$.

experimentally, the n_e radial shift at the outer target is observed by LPs. The simulated electron temperature is, conversely, underestimated at both targets. While LP measurements are prone to underestimate the density and overestimate the temperature at low T_e [5], the DSS measurements are consistent with LPs, in support of the simulations predicting a colder and denser divertor. The heat flux obtained from the IR diagnostics exhibits an in-out asymmetry that is in qualitative agreement with simulations. This asymmetry is stronger in reverse field, as previously observed [6]. Nonetheless, simulations are generally seen to overestimate the target heat flux.

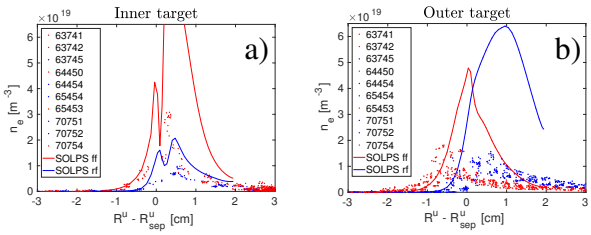

Figure 6: LP electron density at the inner a) and outer b) target in forward (*red*) and reversed field (*blue*). $\langle n_e \rangle_l = 5.1 \cdot 10^{19} m^{-3}$

Conclusions

SOLPS-ITER drift simulations qualitatively reproduce the distribution of divertor heat loads and power fluxes with B_t reversal. The simulated divertor state is, however, colder and denser than in the experiment (LP), resulting in over high carbon radiative emission (DSS), although the total radiation in the SOL is well matched (BOLO). The quantitative discrepancies may indicate an over-estimated ExB drift, which results in stronger in-out asymmetries than experiments. A possible shortcoming of simulations, related to the drift stength, can be in the role of recombination and plasma-neutral interaction, affecting the particle source profile. Future work will extend the comparison to more diagnostics (MANTIS, CXRS, baratrons).

Acknowledgement This work has been carried out within the framework of EUROfusion Consortium and has received funding from the Euratom research and training programme 2014-2018 and 2019-2020 under grant agreement No 633053. The views and opinions expressed herein do not necessarily reflect those of the European Commission. This work was supported in part by the Swiss National Science Foundation and by the US Department of Energy under Award Number DE-SC0010529.

References

[1] X. Bonnin et al, Plasma and Fusion Research **11** 1403102 (2016).

[2] M. Wensing et al., submitted to Physics of Plasmas (2021).

[3] M. Wensing et al., Nucl. Mat. and Energy **25** 100839 (2020)

[4] N. Christen et al., Plasma Phys. Control. Fusion **59**, 105004 (2017)

[5] O. Février et al., Rev. Sci.Instrum. **89**, 053502 (2018)

[6] R. Maurizio et al., Nucl. Fusion **58**, 016052 (2018)